

Measurement of the Flux of Ultrahigh Energy Cosmic Rays from Monocular Observations by the High Resolution Fly's Eye Experiment.

R.U. Abbasi,¹ T. Abu-Zayyad,¹ J.F. Amann,² G. Archbold,¹ J.A. Bellido,³ K. Belov,¹ J.W. Belz,⁴ D.R. Bergman,⁵ Z. Cao,¹ R.W. Clay,³ M.D. Cooper,² H. Dai,¹ B.R. Dawson,³ A.A. Everett,¹ J.H.V. Girard,¹ R.C. Gray,¹ W.F. Hanlon,¹ C.M. Hoffman,² M.H. Holzschneider,² P. Hütemeyer,¹ B.F. Jones,¹ C.C.H. Jui,¹ D.B. Kieda,¹ K. Kim,¹ M.A. Kirn,⁴ E.C. Loh,¹ N. Manago,⁶ L.J. Marek,² K. Martens,¹ G. Martin,⁷ J.A.J. Matthews,⁷ J.N. Matthews,¹ J.R. Meyer,¹ S.A. Moore,¹ P. Morrison,¹ A.N. Moosman,¹ J.R. Mumford,¹ M.W. Munro,⁴ C.A. Painter,² L. Perera,⁵ K. Reil,¹ R. Riehle,¹ M. Roberts,⁷ J.S. Sarracino,² M. Sasaki,⁶ S.R. Schnetzer,⁵ P. Shen,¹ K.M. Simpson,³ G. Sinnis,² J.D. Smith,¹ P. Sokolsky,¹ C. Song,⁸ R.W. Springer,¹ B.T. Stokes,¹ S.F. Taylor,¹ S.B. Thomas,¹ T.N. Thompson,² G.B. Thomson,⁵ D. Tupa,² S. Westerhoff,⁸ L.R. Wiencke,¹ T.D. VanderVeen,¹ A. Zech,⁵ and X. Zhang⁸

(The High Resolution Fly's Eye Collaboration)

¹University of Utah, Department of Physics and High Energy Astrophysics Institute, Salt Lake City, Utah, USA

²Los Alamos National Laboratory, Los Alamos, NM, USA

³University of Adelaide, Department of Physics, Adelaide, South Australia, Australia

⁴University of Montana, Department of Physics and Astronomy, Missoula, Montana, USA.

⁵Rutgers — The State University of New Jersey,

Department of Physics and Astronomy, Piscataway, New Jersey, USA

⁶University of Tokyo, Institute for Cosmic Ray Research, Kashiwa, Japan

⁷University of New Mexico, Department of Physics and Astronomy, Albuquerque, New Mexico, USA

⁸Columbia University, Department of Physics and Nevis Laboratory, New York, New York, USA

We have measured the cosmic ray spectrum above $10^{17.2}$ eV using the two air fluorescence detectors of the High Resolution Fly's Eye observatory operating in monocular mode. We describe the detector, photo-tube and atmospheric calibrations, as well as the analysis techniques for the two detectors. We fit the spectrum to a model consisting of galactic and extra-galactic sources.

The highest energy cosmic rays detected so far, of energies up to and exceeding 10^{20} eV, are very interesting in that they shed light on two important questions: the nature of their origin in astrophysical or other sources and their propagation to us through the Cosmic Microwave Background Radiation (CMBR). The production of pions from interactions of CMBR photons and Ultra High Energy Cosmic Rays (UHECR) is an important energy loss mechanism above $\sim 10^{19.8}$ eV, and produces the Greisen-Zatsepin-K'uzmin (GZK) effect [1, 2]; e^+e^- production in the same collisions is a weaker energy-loss mechanism above a threshold of $10^{17.8}$ eV. We report here the flux of UHECR from $10^{17.2}$ eV to over 10^{20} eV, measured in monocular mode, with the High Resolution Fly's Eye (HiRes) detectors.

The HiRes observatory consists of two air-fluorescence detector sites separated by 12.6 km and located at the U.S. Army Dugway Proving Ground in Utah. Cosmic rays interacting in the upper atmosphere initiate particle cascades known as extensive air-showers. Passage of charged particles excites nitrogen molecules causing emission of (mostly) ultraviolet light. The fluorescence yield has been previously measured by Kakimoto *et al.* [3], and more recently by Nagano *et al.* [4] For this analysis, we used the fluorescence spectrum compiled by Bunner [5] and normalized it to the yield of Kakimoto. By measuring the longitudinal development of the fluorescence signal, one can infer the arrival direction, energy and av-

erage composition of the primary cosmic ray. HiRes was designed to measure the fluorescence light stereoscopically. However our two detectors trigger and reconstruct events independently. In this "monocular" mode our current data have significantly better statistical power and cover a much wider energy range than our stereo sample.

The two HiRes detector sites, referred to as HiRes-I and HiRes-II, are operated on clear, moon-less nights. Over a typical year, each detector accumulates up to 1000 hours of observation. The HiRes-I site has been in operation since June of 1997 [6]. It consists of 21 detector units, each equipped with a 5 m² spherical mirror and 256 photo-tube pixels at its focal plane. Each photo-tube covers a 1° cone of sky. These 21 mirrors cover elevation angles between 3° and 17°. The HiRes-I electronics perform sample-and-hold integration in a 5.6 μ s window, which is long enough to contain signals from all reconstructible events. The HiRes-II site was completed in late 1999 and began observations that year. This site uses the same type of mirrors and photo-tubes as HiRes-I, but contains 42 mirrors, in two rings, covering elevation angles from 3° to 31°. HiRes-II uses an FADC data acquisition system operating at 10 MHz [7]. Both the HiRes-I and -II sites provide 2π azimuthal angle coverage.

To determine the correct shower energies, the air fluorescence technique requires accurate measurement and monitoring of photo-tube gains. Two methods of calibration are used. Pulses from a YAG laser are distributed to

mirrors via optical fibers. They provide a nightly relative calibration. A stable, standard light source is used for a more precise monthly absolute calibration. Overall, the relative photo-tube gains were stable to within 3.5% and the absolute gains were known to $\pm 10\%$ [8].

A second variable in the energy measurement is atmospheric clarity. Light from air showers is attenuated by: (a) molecular (Rayleigh), and (b) aerosol scattering. The former is approximately constant, subject only to small variations in the atmospheric overburden. The aerosol concentration varies with time. HiRes measures the aerosol content by observing scattered light from two steerable laser systems. The laser observed by HiRes-I has been in operation since 1999. The vertical aerosol optical depth from ground to 3.5 km altitude, τ_A , is measured each hour (the vertical transmission through the aerosol is $T = e^{-\tau_A}$). Over two years, these measurements yielded an average τ_A at 355 nm of 0.04 [9]. The RMS of the distribution is 0.02, and the systematic uncertainty in the mean is no larger than this. The average aerosol ground-level horizontal extinction length, Λ_H , was determined to be 25 km. Because about half of our data were collected before the steerable lasers were in operation we used these averages in our analysis and simulation.

Between June 1997 and February 2003, the HiRes-I detector operated for approximately 3600 hours. From this, 2820 hours of good weather data were analyzed. We selected 5.5 million downward, track-like events. For each of these, a shower-detector plane was determined from the pattern of photo-tube hits. We excluded events containing an average number of photo-electrons per photo-tube of less than 25, where fluctuations in signals are too great to permit reliable reconstruction. We also cut out tracks with angular speed in excess of $3.33^\circ/\mu\text{s}$; for these events (typically within 5 km of HiRes-I) the shower maxima appear above the field of view. We selected 12,709 events for reconstruction.

Determination of the shower geometry is possible in monocular mode. The impact parameter, R_p , and the angle of the shower in the plane containing the shower and the detector, ψ , are found by fitting the photo-tube trigger times to the angles at which they view the shower. However, HiRes-I monocular events are too short in angular spread for reliable pure-timing fit. For this analysis, the expected form of the shower development was used to constrain the time fit to yield realistic geometries. The shower profile is assumed to be described by the Gaisser-Hillas parameterization [11], which has been found to be in good agreement with previous HiRes measurements [12] and with CORSIKA/QGSJET simulations [13, 14, 15]. This technique is called the Profile-Constrained Fit (PCF). We allowed the shower maximum, x_m to vary in 35 g/cm² steps between 680 and 900 g/cm², matching the expected range of x_m for proton to iron primaries. After reconstruction, we require a

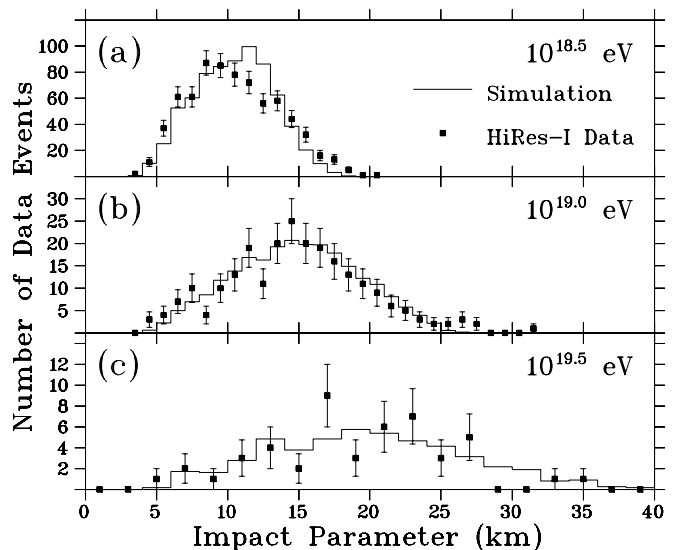


FIG. 1: Comparison of HiRes-I simulated (histogram) and observed (points) R_p distributions at (a) $10^{18.5}$, (b) $10^{19.0}$, and (c) $10^{19.5}$ eV. The Monte Carlo distributions are normalized to the number of data events.

minimum track arc length of 8.0° and a maximum depth for the highest elevation hit of 1000 g/cm². Significant contamination from the forward-beamed direct Čerenkov light degrades the reliability of the PCF. Therefore, we rejected tracks with $\psi > 120^\circ$ and those with two or more angular bins of the shower with $>25\%$ Čerenkov light. A total of 6,920 events remained.

Monte Carlo studies were performed to assess the reliability of the PCF method. The simulated events were subjected to the same selection criteria and cuts imposed on the data. An RMS energy resolution of better than 20% was seen above $10^{19.5}$ eV. However, the resolution degrades at lower energies to about 25% at $10^{18.5}$ eV. These Monte Carlo results were cross-checked by examination of a smaller set of stereo events where the geometry is more precisely known. Comparing the energies reconstructed using monocular and stereo geometries, we obtained resolutions similar to those seen in simulation.

The simulation is also used to calculate the aperture. To verify the reliability of this calculation, we compared Monte Carlo distributions of many geometrical and physical variables to the actual data, and consistently found good agreement. The Monte Carlo predictions for the zenith angle and impact parameter (R_p), in particular, are sensitive to the detector operating parameters. We use input parameters representative of actual running conditions, and again see good agreement between data and simulation. For example, we show the comparison of R_p distribution at three energies in Figure 1.

The analysis of HiRes-II monocular data was similar to that for HiRes-I. The data sample was collected during 142 hours of good weather between Dec. 1999 and

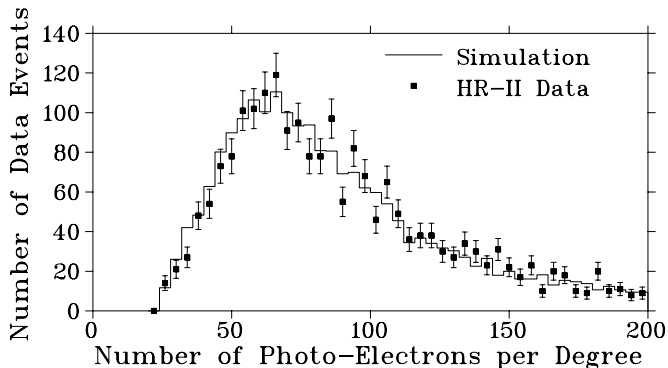


FIG. 2: A comparison of the number of photo-electrons per degree of track seen in HiRes-II monocular events (data points) and in simulation (histogram).

May 2000. This period represents the first stable running of the HiRes-II detector. At the end of this period, a considerable change was made in the trigger, so that subsequently collected data will be analyzed separately. With the greater elevation coverage at HiRes-II, it was feasible to reconstruct the shower geometry from timing alone (the PCF is unnecessary). Therefore we were able to loosen some cuts for the HiRes-II fits. At this stage 104,048 downward-going events remained.

With the geometry of the shower known, we fit the measured shower profile to the Gaisser-Hillas parameterization [11]. The events were required to have a good fit to the Gaisser-Hillas function, to have a track length greater than 10° for upper ring or multi-mirror events, a track length greater than 7° for lower ring events, an angular speed less than $11^\circ/\mu\text{s}$ (the larger cut for HiRes-II reflects its extended elevation coverage), a zenith angle less than 60° , and a shower maximum visible in our detector. There was also a cut on the size of the Čerenkov light subtraction at $< 60\%$ of signal. Again, the same selections and cuts were applied to both simulated and real events. There were 781 events left after these cuts. These simulations also gave excellent reproduction of the data, as seen, for example, in the comparison of the number of photo-electrons per degree of track in Fig. 2.

For both HiRes-I and HiRes-II events, the photo-electron count was converted to a shower size at each atmospheric depth, using the known geometry of the shower, and corrected for atmospheric attenuation. We integrated the resulting function over x and then multiplied by the average energy loss per particle to give the visible shower energy. A correction for energy carried off by non-observable particles to give the total shower energy ($\sim 10\%$) [13] was then applied.

The monocular reconstruction apertures are shown in Fig. 3. Both approach $10^4 \text{ km}^2\text{sr}$ above 10^{20} eV . We restrict our result for HiRes-I to energies $> 10^{18.5} \text{ eV}$; below this the PCF technique is unstable. Due to longer tracks and additional timing information, the RMS energy res-

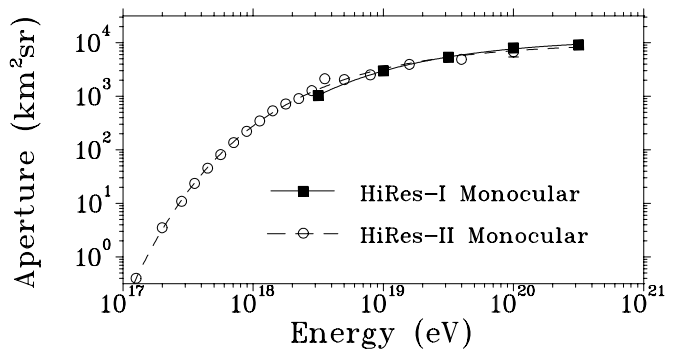


FIG. 3: Calculated HiRes monocular Reconstruction aperture in the energy range $10^{17} - 10^{20.5} \text{ eV}$. The HiRes-I and II apertures are shown by the squares and circles, respectively.

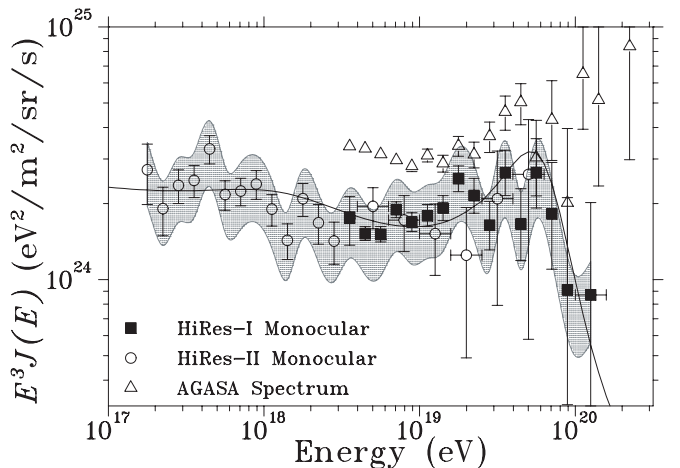


FIG. 4: Combined HiRes monocular spectrum. The squares and circles represent the HiRes-I and II differential flux $J(E)$, multiplied by E^3 . The error bars are statistical only, and the systematic uncertainties are indicated by the shaded region. The line is a fit to the data of a model, described in the text, of galactic and extra-galactic cosmic ray sources. The AGASA spectrum [16] is shown by triangles for comparison.

olution for HiRes-II remains better than 30% down to $10^{17.2} \text{ eV}$. However, the HiRes-II data become statistically depleted above 10^{19} eV .

We calculated the cosmic ray flux for HiRes-I above $10^{18.5} \text{ eV}$, and for HiRes-II above $10^{17.2} \text{ eV}$. This combined spectrum is shown in Fig. 4, where the flux $J(E)$ has been multiplied by E^3 . The error bars represent the 68% confidence interval for the Poisson fluctuations in the number of events. The HiRes-I flux is the result of two independent analyses [17, 18].

The largest systematic uncertainties in the energy scale are the absolute calibration of the photo-tubes ($\pm 10\%$) [8], the fluorescence yield ($\pm 10\%$) [3, 4], and the correction for unobserved energy in the shower ($\pm 5\%$) [13, 19]. Excluding atmospheric effects, the energy scale uncertainty is $\pm 15\%$. This translates to a systematic uncertainty in the flux, $J(E)$, of $\pm 27\%$.

We estimate the atmospheric contribution to the energy error by repeating the event reconstruction with τ_A varied by ± 1 RMS value, from 0.04 to 0.06 and 0.02. While a ± 0.02 change in τ_A represents a $\pm 50\%$ change in aerosol concentration, that contribution to the attenuation at these levels is small, and a 0.02 change modifies the transmission by only $\sim 10\%$ at 25 km from the detector. We found the reconstructed geometries of HiRes-I events above $10^{18.5}$ eV to be insensitive to changes in assumed τ_A , and we saw a maximum change in the energy of $\pm 13\%$ at 10^{20} eV, decreasing to $\pm 6\%$ at $10^{18.5}$ eV. The geometries of the HiRes-II events do not depend on τ_A at all, and the change in energy scale for these are typically 6% or less. Taking the HiRes-I average energy shift, 9%, the overall systematic uncertainty in energy scale, including atmospheric effects, then becomes $\pm 17\%$.

We also recalculated the aperture and the flux with τ_A changed by ± 0.02 . From these we obtained an average atmospheric uncertainty in $J(E)$ of $\pm 15\%$, and an uncertainty in the flux of $\pm 31\%$. The overall systematic uncertainties in the flux, including the energy-dependent atmospheric contribution (with a slope in $|\Delta J(E)|$ of about 5% per decade of energy) are indicated by the shaded region in Figure 4. The relative calibration uncertainty between the two detector sites is less than 10%.

Our data contain two events at or above 10^{20} eV, measured at 1.0 and 1.5×10^{20} eV. Assuming a purely molecular atmosphere ($\tau_A = 0.0$), we obtain lower energy limits of 0.9 and 1.2×10^{20} eV. In the energy range where both detectors' data have good statistical power, the results agree with each other very well. However, our flux values are on average 13% lower than the stereo spectrum reported by Fly's Eye [20]. This difference can be explained by a 7% offset in the energy calibration alone, well within the stated uncertainty of the two experiments.

The GZK effect predicts a suppression in the UHECR flux above $10^{19.8}$ eV. We fit our data to a model consisting of galactic and extra-galactic sources [21], that includes the GZK effect. We use the extra-galactic source model of Berezhinsky *et al.* [22], where we assume a uniform (over the Universe) proton source distribution with a maximum at-source energy of 10^{21} eV, and a galactic spectrum consistent with observations that the composition changes from heavy to light near 10^{18} eV. The χ^2 of this fit is 48.5 for 37 degrees of freedom, and the fit is shown in Fig. 4. Details can be found in [23]. In this model the fall-off above $\log E$ of 19.8 is due to crossing the pion production threshold, and the second knee comes from e^+e^- pair production pile-up.

For comparison, the published AGASA spectrum [16] is shown in Fig. 4. Compared to the HiRes monocular spectrum, the AGASA flux values are about 60-70% higher. The AGASA data contain 11 events above

10^{20} eV and 24 above $10^{19.8}$ eV, with an integrated exposure of $\sim 1.0 \times 10^3$ km²sr-yr. The HiRes data have two events at or above 10^{20} eV, and 10 above $10^{19.8}$ eV, with exposures of 2.4 and 2.2×10^3 km²sr-yr. at these two energies. If we were to increase the HiRes energy scale by 17% (one RMS systematic deviation), the number of events above 10^{20} , and $10^{19.8}$ eV would become three and 20. A decrease in energy scale of 17% changes these numbers to one and 6.

This work is supported by US NSF grants PHY-9321949 PHY-9974537, PHY-9904048, PHYS-0245428, PHY-0140688, by the DOE grant FG03-92ER40732, and by the Australian Research Council. We gratefully acknowledge the contributions from the technical staffs of our home institutions and the Utah Center for High Performance Computing. The cooperation of Colonels E. Fischer and G. Harter, the US Army, and the Dugway Proving Ground staff is greatly appreciated.

-
- [1] K. Greisen, Phys. Rev. Lett. **16**, 748, (1966).
 - [2] G.T. Zatsepin and V.A. K'uzmin, Pis'ma Zh. Eksp. Teor. Fiz. **4**, 114 (166) [JETP Lett. **4**, 78 (1966)].
 - [3] F. Kakimoto *et al.*, NIM **A372**, 527 (1996).
 - [4] M. Nagano *et al.*, astro-ph/0303193, to be published in Astropart. Phys.
 - [5] A.N. Bunner, Ph.D. Thesis (Cornell University) (1967).
 - [6] T. Abu-Zayyad *et al.*, Proc. 26th ICRC (Salt Lake City), **5**, 349, (1999).
 - [7] J. Boyer *et al.*, NIM **A482**, 457 (2002).
 - [8] T. Abu-Zayyad *et al.*, to be submitted to NIM.
 - [9] T. Abu-Zayyad *et al.*, in preparation, and <http://www.cosmic-ray.org/atmos/>.
 - [10] R.M. Baltrusaitis *et al.*, NIM **A240**, 410 (1985).
 - [11] T. Gaisser and A.M. Hillas, Proc. 15th ICRC (Plovdiv), **8**, 353, (1977).
 - [12] T. Abu-Zayyad *et al.*, Astropart. Phys. **16**, 1, (2001).
 - [13] C. Song, Z. Cao *et al.*, Astropart. Phys. **14**, 7, (2000).
 - [14] D. Heck, *et al.* Report FZKA 6019 (1998), Forschungszentrum Karlsruhe.
 - [15] N.N. Kalmykov, S.S. Ostapchenko and A.I. Pavlov, Nucl. Phys. B (Proc. Suppl.) **52B**, 17, (1997).
 - [16] M. Takeda *et al.*, Astropart. Phys. **19**, 447, (2003).
 - [17] T. Abu-Zayyad, Ph.D Thesis, University of Utah (2000).
 - [18] X. Zhang, Ph.D Thesis, Columbia University (2001).
 - [19] J. Linsley, Proc. 18th ICRC (Bangalore), **12**, 135, (1983).
 - [20] D.J. Bird *et al.*, Phys. Rev. Lett. **71**, 3401, (1993).
 - [21] E. Waxman, Astrophys.J.Lett. 452, L1 (1995), J.N. Bahcall & E. Waxman, Phys.Lett. **B556** (2003) 1-6.
 - [22] V. Berezhinsky, A.Z. Gazizov, and S.I. Grigorieva, hep-ph/0204357, Scully and Stecker 2002, Astropart. Phys. **16**, 271.
 - [23] T. Abu-Zayyad *et al.*, astro-ph/0208301, submitted to Astropart. Phys.